Supporting Information

Efficient and selective DNA modification on bacterial membranes

Qian Tian, Yousef Bagheri, Puspam Keshri, Rigumula Wu, Kewei Ren, Qikun Yu, Bin Zhao, and Mingxu You*

Department of Chemistry, University of Massachusetts, Amherst, Massachusetts 01003, USA

*e-mail: mingxuyou@chem.umass.edu

1. Materials and Methods

Chemicals and reagents. Unless specified, all the chemicals were purchased from Sigma or Fisher Scientific and directly used without further purification. DNA strands with only fluorophore labeling were ordered from Integrated DNA Technology. DNAs on controlled pore glass beads or with tetraethylene glycol (TEG)–cholesterol modification were ordered from Yale Keck Oligonucleotide Synthesis. 1,2-dilauroyl-*sn*-glycero-3-phosphocholine (DLPC) was purchased from Avanti Polar Lipids. 1,1-didodecyl-3,3,3,3-tetramethylindocarbocyanine perchlorate (DiI C12 perchlorate) was purchased from AAT Bioquest.

Synthesis of 16:0-16:0 phosphoramidite. The 16:0-16:0 phosphoramidite was synthesized by following a previous report[1]. Briefly, palmitoyl acid was dissolved in ice-cooled anhydrous dichloromethane (DCM) and the mixture of oxalyl chloride and catalytic amount of dimethylformamide (DMF) was added to the palmitoyl acid dropwise (palmitoyl acid: oxalyl chloride=1:2). The reaction mixture was stirred on ice for 2 h and then vacuumed to remove excess oxalyl chloride. The synthesized palmitoyl chloride was dissolved in dichloroethane (DCE) and added to 1,3-diamino-2-dydroxypropane in the presence of trimethylamine (TEA). The palmitoyl chloride and TEA were 2.3~2.4-fold more than 1,3-diamino-2-dydroxypropane. The reaction was stirred at room temperature for 2 h and then at 70ºC in an oil bath for overnight. Next day, the solid was washed by cold DCM, methanol, 5% sodium bicarbonate and acetone until the organic phase was totally separated from aqueous phase. The crude 16:0-16:0 fatty acid was further purified with column chromatography. The purified 16:0-16:0 fatty acid was then dissolved in ice cold DCM in the presence of diisopropylethylamine (DIPEA). 2-cyanoethyl-N,N'-diisopropylchlorophosphoramidite in DCM was then added in a dropwise manner. The reaction mixture was stirred at room temperature for 1 h and 60ºC for 2 h. The final product (16:0-16:0 phosphoramidite) was then purified with column chromatography. ^{1}H-NMR (400 MHz, $CDCl_3$): δ (ppm) 0.9 (t, 6H), 1.2-1.4 (m, 64H), 1.6 (m, 4H), 2.2 (t, 4H), 2.6 (t, 2H), 2.8-3.1 (m, 2H), 3.6 (m, 2H), 3.8 (m, 2H), 3.9 (m, 2H). ^{13}C NMR (100 MHz, $CDCl_3$): δ (ppm) 174.68, 118.45, 71.14, 58.42, 43.50, 40.89, 37.05, 32.22, 26.51, 21.42, 14.23. ^{31}P NMR (162 MHz, $CDCl_3$): δ (ppm) 148. ESI-MS: ($C_{44}H_{87}N_4O_4P + Na^+$) calculated, 789.65; found, 788.5922.

Synthesis of 18:1-18:1 phosphoramidite. The synthesis of 18:1-18:1 phosphoramidite was similar as that of 16:0-16:0. Briefly, oleoyl chloride was dissolved in DCE and added into 1,3-diamino-2-dydroxypropane in the presence of TEA. The mixture was stirred at room temperature for 2 h and then 70ºC overnight. After cooling down and washing with cold DCM, methanol, 5% sodium bicarbonate and acetone, the raw 18:1-18:1 fatty acid was purified using column chromatograph. Then, the purified fatty acid was dissolve in cold DCM with DIPEA. 2-cyanoethyl-N,N'-diisopropylchloro-phosphoramidite in DCM was added in a dropwise manner. After 1 h reaction at room temperature and 2 h at 60ºC with stirring, the mixture was further purified using column chromatography. ^{1}H-NMR (400 MHz, $CDCl_3$): δ (ppm) 0.9 (t,6H), 1.2-1.5 (m, 44H), 1.6 (m, 4H), 2.1 (m, 8H), 2.4 (t, 4H), 3.1 (m, 2H), 3.4 (d, 4H), 5.4 (m, 4H). ^{13}C NMR (100 MHz, $CDCl_3$): δ (ppm) 174.99, 129.89, 118.3, 77.36, 69.90, 57.18, 40.62, 36.58, 32.44, 29.32, 27.31, 22.16, 14.62. ^{31}P NMR (162MHz, $CDCl_3$): δ (ppm) 147. ESI-MS: ($C_{48}H_{91}N_4O_4P + Na^+$) calculated, 842.25; found, 842.6072.

Synthesis of 18:0-18:0 phosphoramidite. Similarly, 18:0-18:0 phosphoramidite was synthesized. In short, stearic chloride was dissolved in cold DCM. A mixture of 1,3-diamino-2-dydroxypropane and

TEA was then added to stearic chloride dropwise and stirred at room temperature for 2 h and 70ºC overnight. The raw 18:0-18:0 fatty acid was cooled down and washed with cold DCM, methanol, 5% sodium bicarbonate and acetone. After purified with column chromatography, the dried fatty acid was dissolved in cold DCM in the presence of DIPEA. 2-cyanoethyl-N,N'-diisopropylchlorophosphoramidite in DCM was mixed with it dropwise. The reaction mixture was stirred for 1 h at room temperature and 2 h at 60ºC. The final product was then purified using column chromatography. ^{1}H-NMR (400 MHz, $CDCl_3$): δ (ppm) 0.9 (t, 6H), 1.2-1.4 (m, 72H), 1.6 (m, 4H), 2.2 (t, 4H), 2.6 (t, 2H), 2.8-3.1 (m, 2H), 3.6 (m, 2H), 3.8 (m, 2H), 3.9 (m, 2H). ^{13}C NMR (100 MHz, $CDCl_3$): δ (ppm) 174.4, 118.16, 70.70, 58.18, 43.11, 40.37, 36.40, 30.01, 24.32, 21.13, 14.41. ^{31}P NMR (162 MHz, $CDCl_3$): δ (ppm) 147. ESI-MS: ($C_{48}H_{95}N_4O_4P + Na^+$) calculated, 846.29; found, 845.6390.

Synthesis of lipid-DNA conjugates. The conjugation of lipid with oligonucleotide was performed following the protocol from a previous report[1]. Briefly, 500 µL of 200 mM lipid phosphoramidite was mixed with freshly made 1 mL of 5-(ethylthio)-1H-tetrazole (ETT) in DCM. The mixture was loaded into a syringe with a conjugation column containing 200 nmol of DNA on controlled pore glass beads, and reacted for 15 min. After oxidizing with an iodine solution, the lipid-modified DNAs were cleaved from the beads with ammonia for 2 h at 37ºC with shaking. These lipid-DNA conjugates were further purified in a reversed phase HPLC with a C4 column. The eluent used for purification contained acetonitrile with 100 nM triethylammonium acetate buffer (pH=7.5), running from 10% to 100% in 30 min.

Bacterial strains and cell culture. The bacterial strains used in this paper include *Escherichia coli (*E. coli) TOP10, *Escherichia coli (*E. coli) BL21 (DE3)*, *Staphylococcus aureus* (S. aureus) WT, *Corynebacterium glutamicum* (C. glutamicum) ATCC 13032 WT, *Micrococcus luteus (M. luteus)*, and *Pseudomonas aeruginosa (P. aeruginosa) PO1.* All the strains were grown in the LB media at 37ºC with shaking at 200 rpm, and for C. glutamicum, 2% of glucose was supplemented to LB media. Streptomycin and ampicillin was added for growing *E. coli* TOP10 and BL21. To induce the red fluorescent protein expression in the BL21 cells, 1 mM IPTG was added for 1 h when the optical density at 600 nm was reached to 0.4–0.6. After the growth, the bacteria were centrifuged down at 5,000 rpm for 2 min and the cell pellets were suspended with DPBS and coated onto the glass bottom of 8-well chambers, which have been pretreated with poly-L-lysine for imaging.

Cell imaging and data analysis. After coating on the glass bottom imaging chamber, the bacteria were incubated with the lipid-DNA conjugates at different temperature for different period of time. The free lipid-DNA conjugates were then washed away with DPBS for 3 times before proceeding to take fluorescence images. Here, no washing was performed for the kinetic and membrane persistence studies. Most images were collected with an NIS-element AR software using a Nikon TiE microscope with Yogokawa spinning disk confocal. To characterize more detailed membrane modification signals, a super-resolution Nikon TiE structure illumination microscope with A1 resonant scanning confocal was used. The analysis of fluorescence intensities was performed with an NIS-element AR Analysis software and ImageJ. Raw data from the NIS-element analysis software was further processed using the Origin, GraphPad Prism, and SYSTAT software.

Preparation of supported lipid bilayer (SLB). To prepare SLB, we need to first prepare lipid vesicles. Here, 1,2-dilauroyl-*sn*-glycero-3-phosphocholine (DLPC) was first dissolved in chloroform (10 mg/ml), and 40 µL (0.4 mg) of DLPC solution was added in a round-bottom flask. The DLPC was then air-dried

and vacuumed for 1 h to remove all the chloroform. The dried DLPC was suspended in 1 mL PBS by vortexing and then frozen in liquid nitrogen and thawed in a 37ºC water bath for 3 min. The freeze-thaw cycle was repeated for 5 times to break the multilamellar liposomes into unilamellar vesicles[2]. Finally, these treated DLPC was extruded through a 0.1 μm membrane to obtain lipid vesicles of uniform sizes. The size of the lipid vesicles was measured based on their dynamic light scattering at room temperature using a Malvern Nanozetasizer.

To prepare SLB, the glass bottom of a 96-well plate was first treated with freshly made 2 M NaOH solution for 1 h for cleaning. The NaOH was completely washed away with deionized water for 30 times. 50 μL of lipid vesicles was added to these pre-cleaned wells and incubated for 45 min. After washing with PBS for 15 times to remove free vesicles, 20 μL of 0.1% BSA was added for 20 min and then washed away with PBS for 15 times. The lipid-DNA conjugates were then added, incubated for 20 min, and washed with PBS for 3 times before imaging. The imaging condition of these SLB-anchored lipid-DNA conjugates was exactly the same as that for the cell imaging.

Linear discriminant analysis. The clustering of different bacterial strains and MDCK cells were performed with a linear discriminant analysis using an SYSTAT software (version 13.2). The raw fluorescence intensity of the lipid-DNA conjugates on different cell membranes were normalized based on the highest fluorescence intensity collected and then processed by SYSTAT. The normalized fluorescence response patterns were transformed to the canonical score with a 0.001 tolerance set. Finally, the canonical scores were plotted into the shown scatterplots.

2. Supplementary Figures

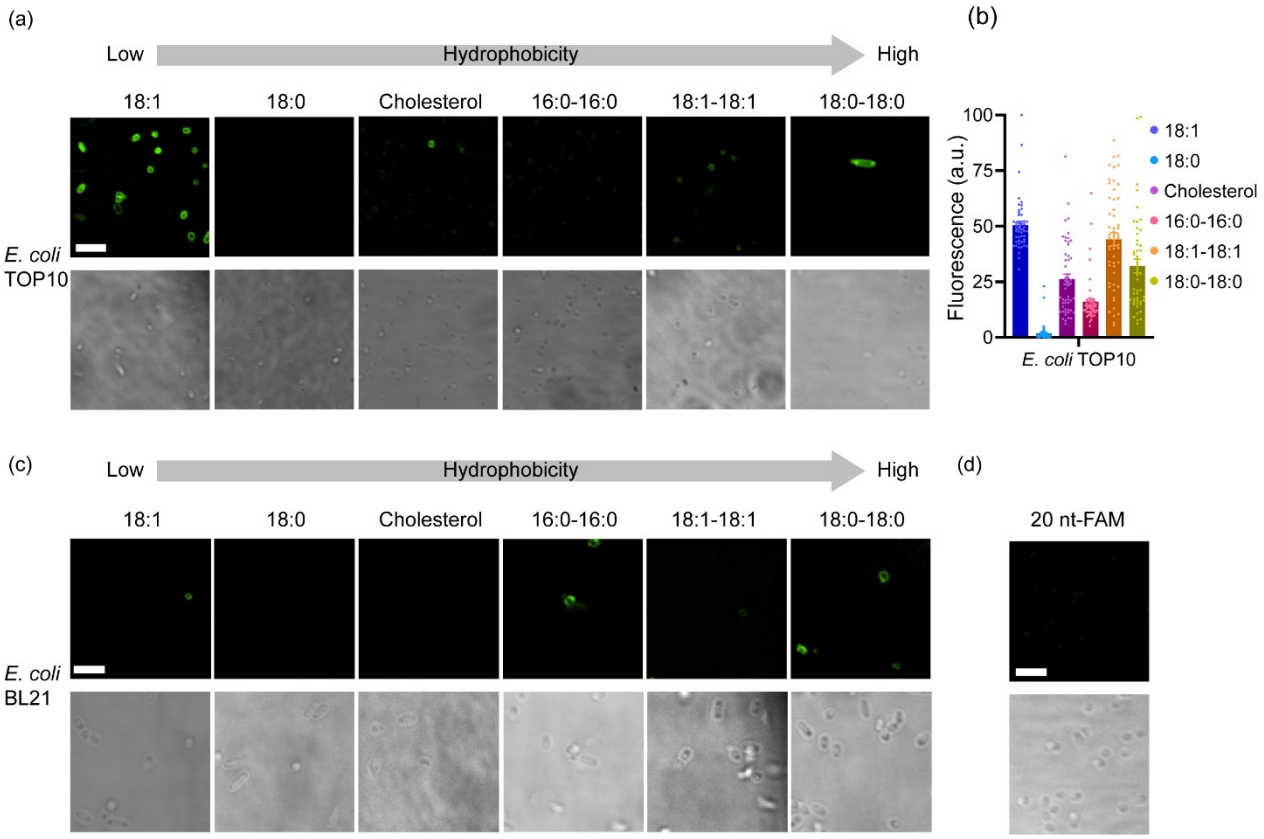

Figure S1. (a) Fluorescence imaging of the lipid-DNA insertion onto the membranes of *E. coli* TOP10 cells. Images were taken after 1 μM conjugate was incubated with TOP10 cells for 1 h at 37ºC. (b) Fluorescence distributions on individual TOP10 cell membranes after 1 h incubation at 37ºC with 1 μM of each lipid-DNA conjugate. These fluorescence intensities were normalized to the maximum cellular fluorescence observed. At least 50 cells were analyzed in each case from different regions of imaging. (c) Fluorescence imaging of the lipid-DNA insertion onto the membranes of *E. coli* BL21 cells. Images were taken after 1 μM conjugate was incubated with BL21 cells for 1 h at 37ºC. (d) Fluorescence imaging of TOP10 cells after 1 h incubation at 37°C with 1 μM of a FAM-modified 20 nt DNA. Scale bar: 5 μm.

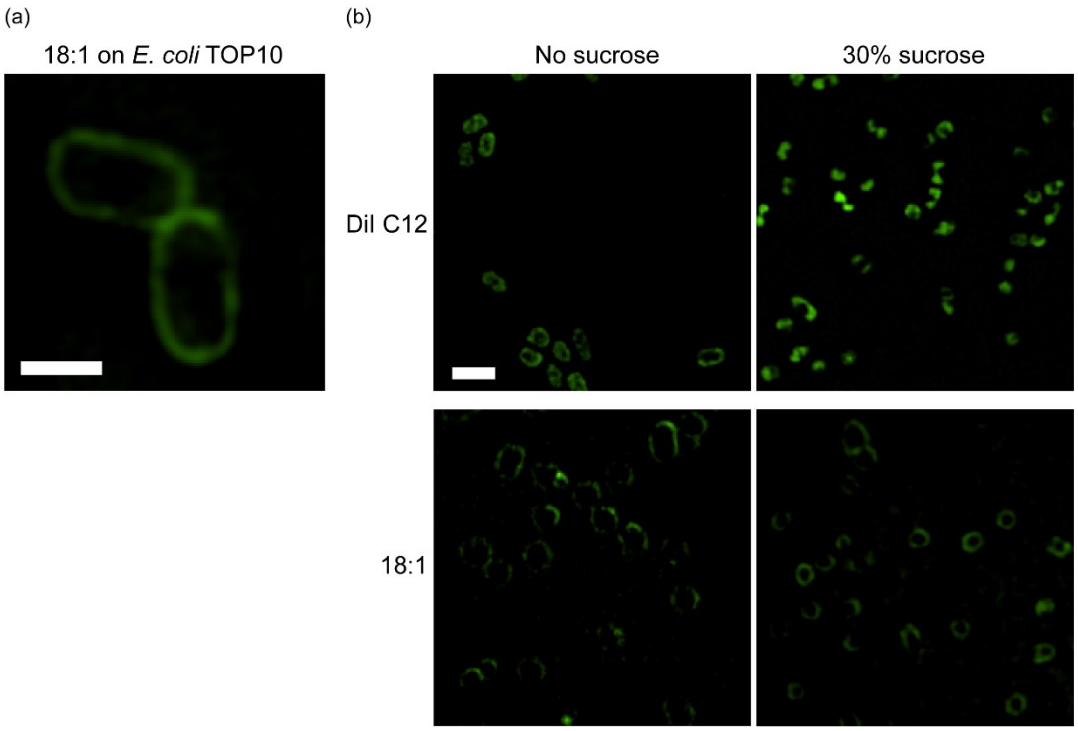

Figure S2. (a) Structured illumination microscopy imaging of the 18:1-DNA conjugate on the membranes of *E. coli* TOP10 cells. Cells were incubated with 1 μM of the conjugate at 37°C for 1 h. Scale bar, 1 μm. (b) Sucrose-induced plasmolysis of (top) DiI-C12- and (bottom) 18:1-DNA-conjugate-stained TOP10 cells. Here, these TOP10 cells were first incubated with 5 μg/mL DiI-C12 or 2 μM 18:1-DNA at 37ºC for 1 h, and then 30% sucrose-supplemented M9 medium was added for 3 min. Scale bar, 2 μm.

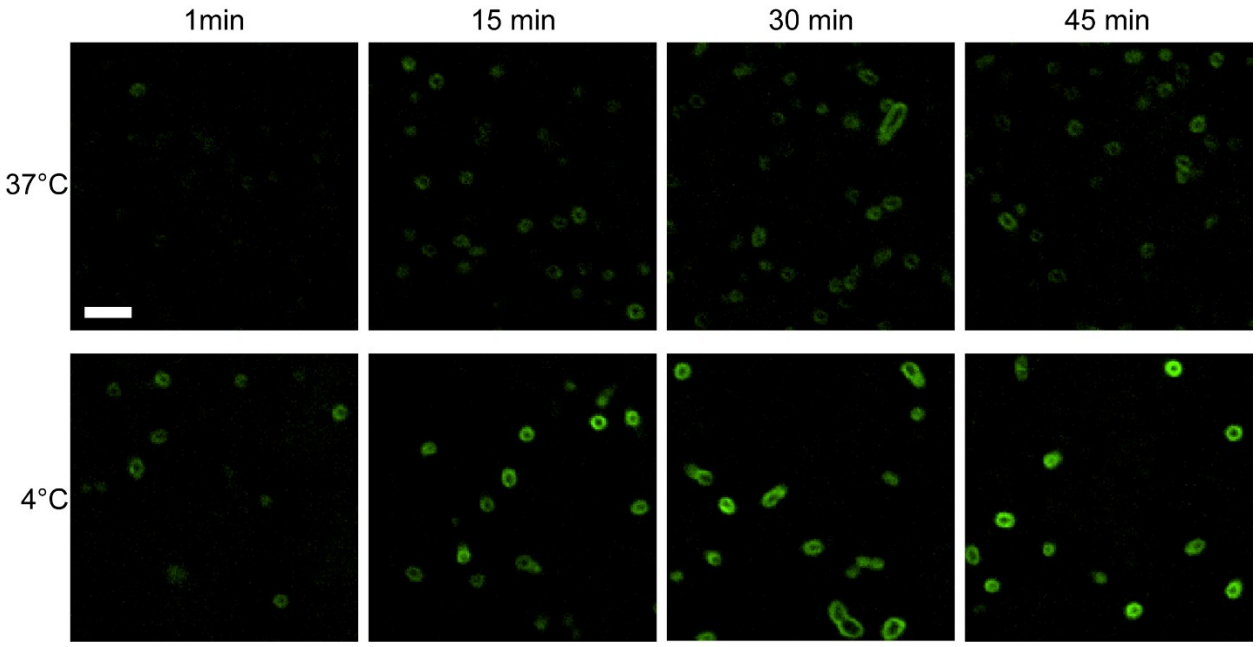

Figure S3. Fluorescence imaging of the membrane insertion kinetics of the 18:1-DNA conjugate onto *E. coli* TOP10 cells. At 0 min, 1 μM 18:1-DNA conjugate was added at either 37°C or 4°C. Scale bar, 5 μm.

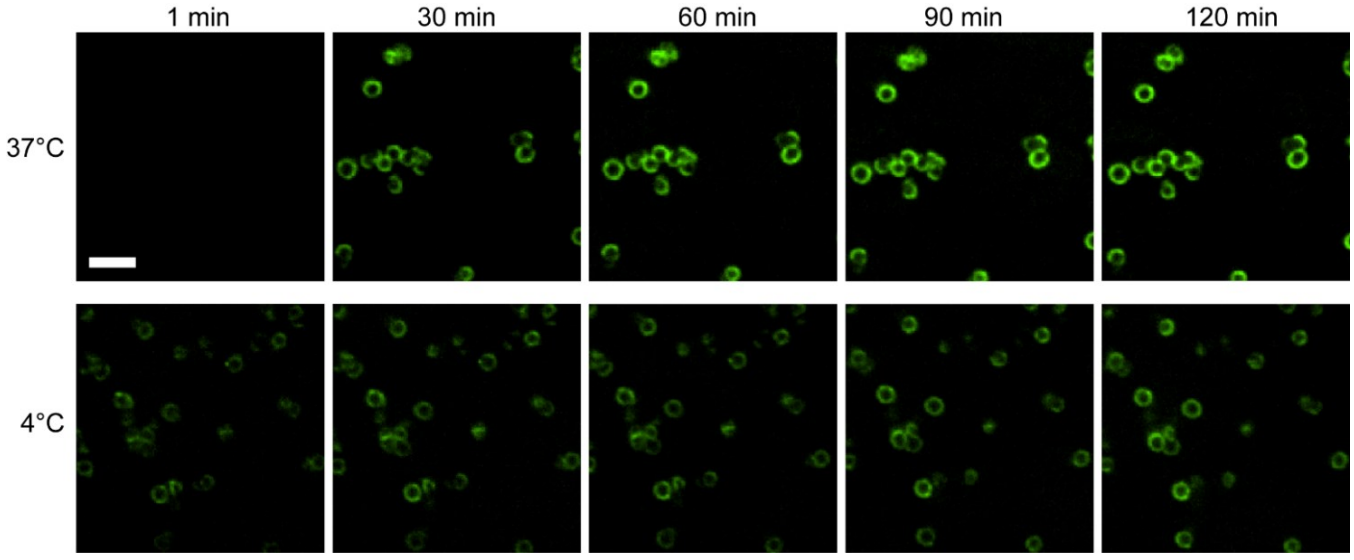

Figure S4. Fluorescence imaging of the membrane insertion kinetics of the 16:0-16:0-DNA conjugate onto *S. aureus* cells. At 0 min, 1 μM 16:0-16:0-DNA conjugate was added at either 37°C or 4°C. Scale bar, 5 μm.

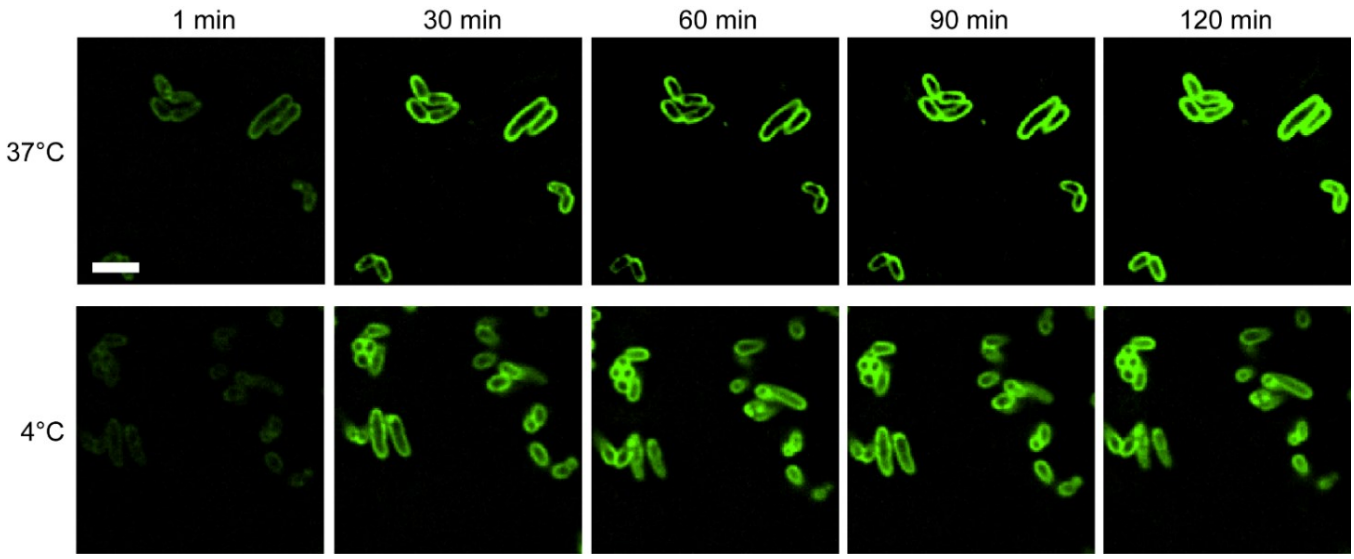

Figure S5. Fluorescence imaging of the membrane insertion kinetics of the 16:0-16:0-DNA conjugate onto *C. glutamicum* cells. At 0 min, 1 μM 16:0-16:0-DNA conjugate was added at either 37°C or 4°C. Scale bar, 5 μm.

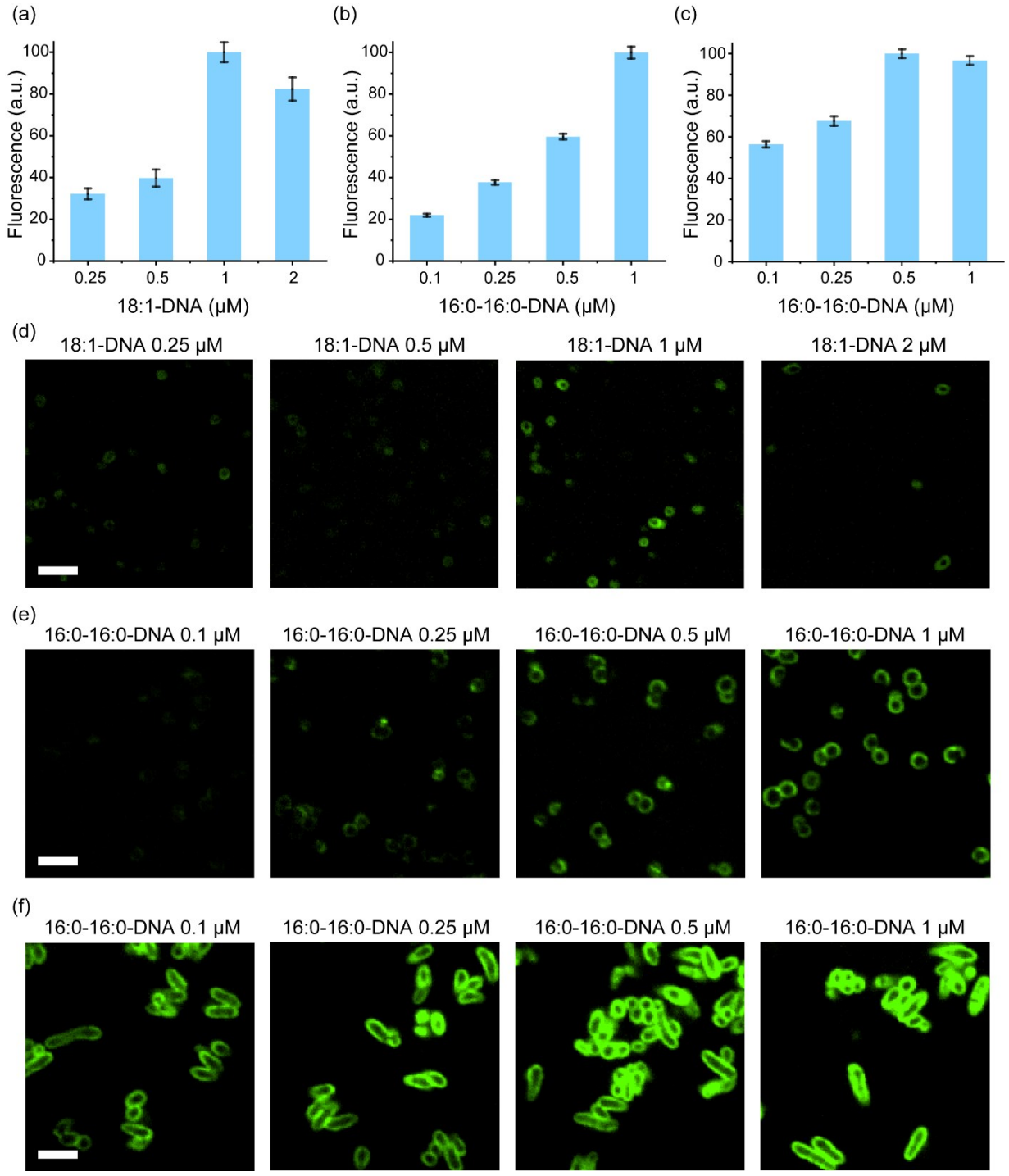

Figure S6. (a, d) Normalized membrane fluorescence intensities and representative images of *E. coli* TOP10 cells after incubating with different initial concentrations of the 18:1-DNA conjugate at 37°C for 45 min. (b, e) Normalized membrane fluorescence intensities and representative images of *S. aureus* cells after incubating with different initial concentrations of the 16:0-16:0-DNA conjugate at 37°C for 1 h. (c, f) Normalized membrane fluorescence intensities and representative images of *C. glutamicum* cells after incubating with different initial concentrations of the 16:0-16:0-DNA conjugate at 37°C for 1 h. Error bars represent the standard error of the mean values as analyzed from at least 50 cells in each case from different regions of imaging. Scale bar, 5 μm.

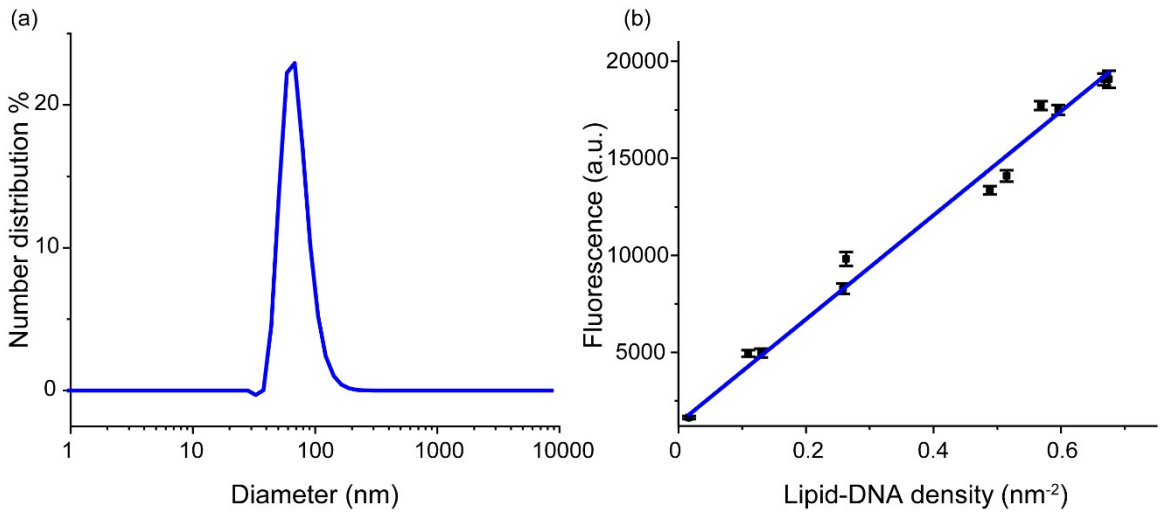

Figure S7. (a) Dynamic light scattering measurement of the size distributions of the DLPC unilamellar vesicles. The measurement was performed at room temperature with 643 μM vesicles from three trials. (b) Standard calibration curve to correlate the fluorescence intensity with the lipid-DNA conjugate density on the supported lipid bilayer. Error bars represent the standard error of the mean values as measured from at least 100 regions of imaging.

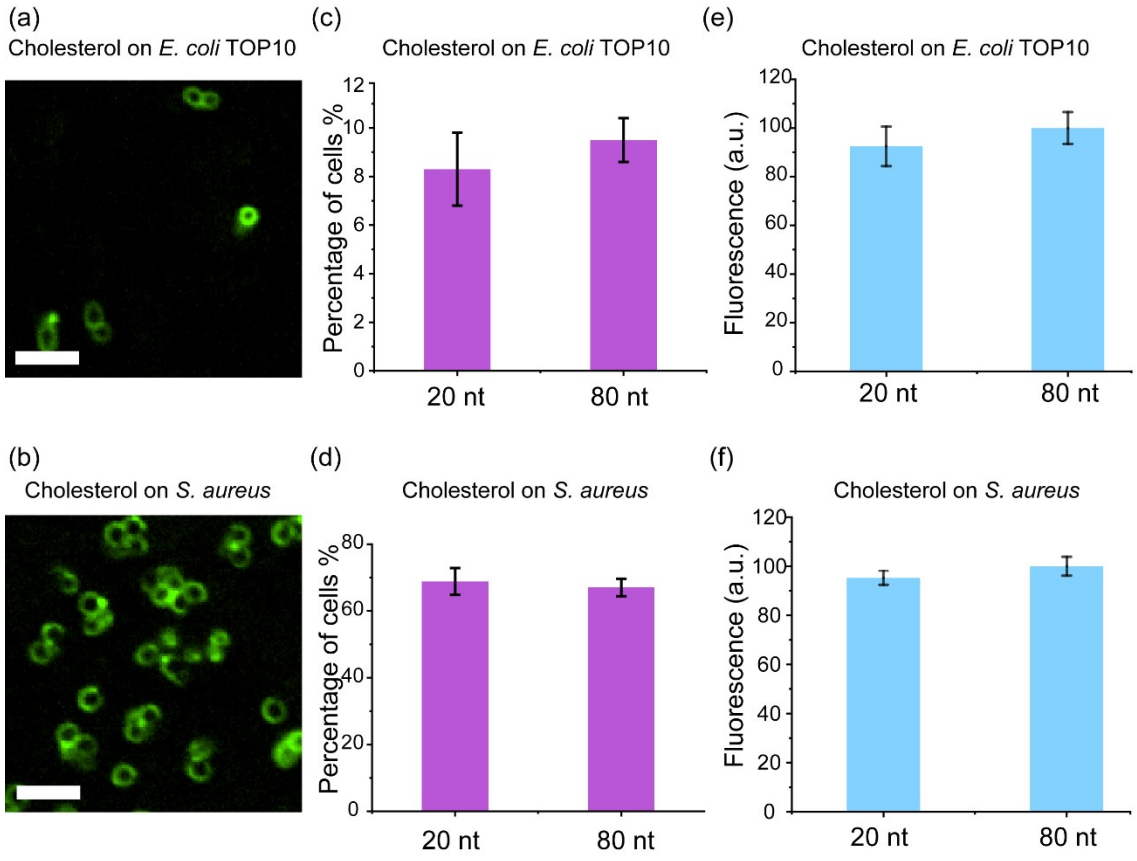

Figure S8. (a, b) Fluorescence imaging of the membrane insertion of 1 μM 80 nt DNA-lipid conjugate onto (a) *E. coli* TOP10 cells and (b) *S. aureus* cells after 1 h incubation at 37ºC. Scale bar, 5 μm. (c, d) (c, d) Modification efficiency of 1 μM of 20 nt and 80 nt-cholesterol probes on the (c) *E. coli* TOP10 cells and (d) *S. aureus* cells after 1 h incubation at 37ºC. Shown was the percentage of cells exhibited fluorescence intensity larger than two-fold of cellular autofluorescence background. At least 100 cells were analyzed in each case. (e, f) Normalized fluorescence intensities of 20 nt and 80 nt-based cholesterol-DNA conjugates on the membrane of (e) *E. coli* TOP10 and (f) *S. aureus* cells. Error bars represent the standard error of the mean values as analyzed from at least 40 cells with high modification efficiency in each case from different regions of imaging.

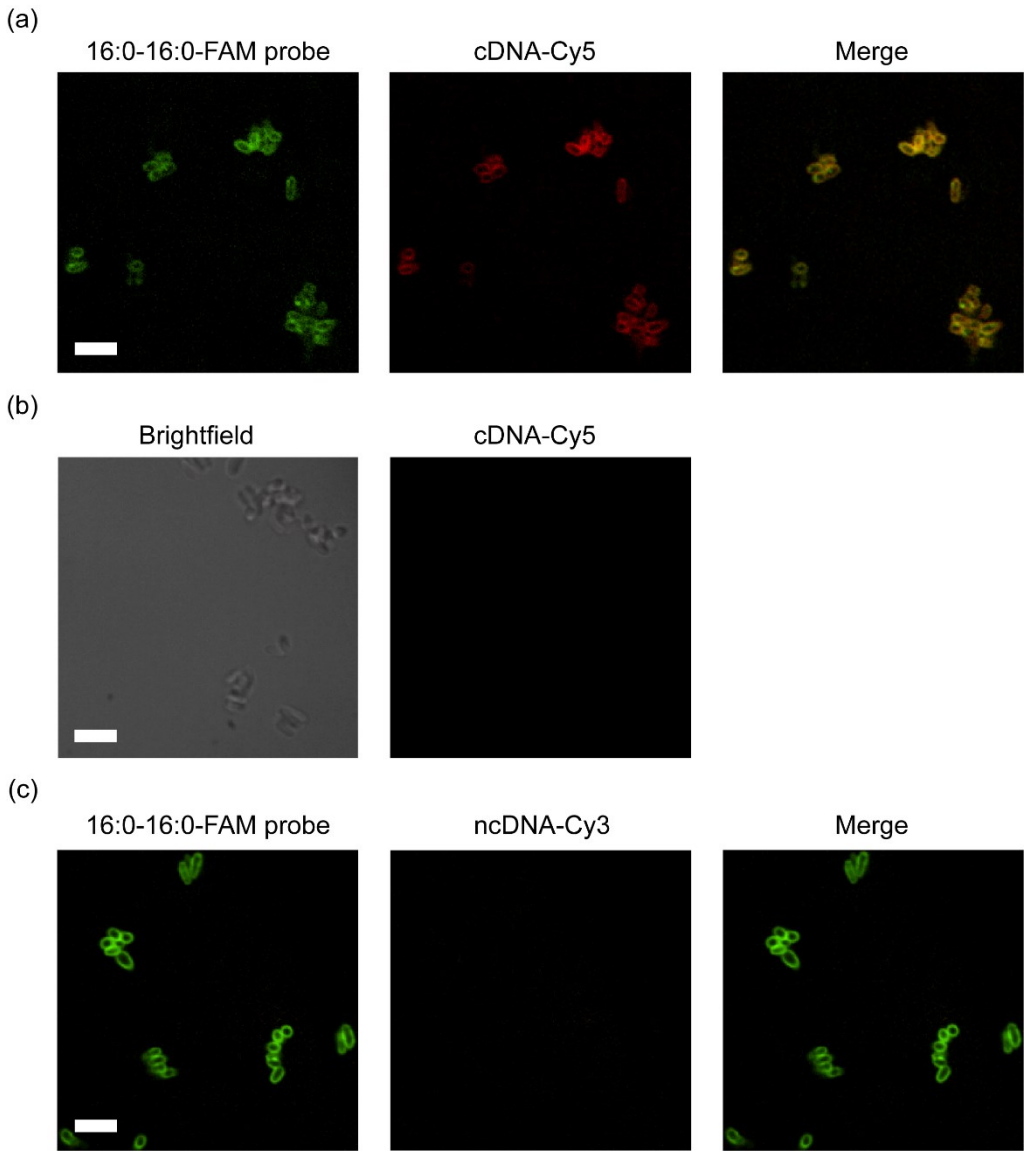

Figure S9. (a) Colocalization of the FAM-labeled 16:0-16:0-DNA conjugate with a Cy5-labelled complementary strand on the membrane of *C. glutamicum* cells. These cells were first incubated with 0.5 μM of the 16:0-16:0-DNA conjugate for 1 h at 37°C, after washing away the free probes, 1 μM complementary strand was then added and incubated for 30 min. The Pearson correlation coefficient was determined to be 0.76. (b) Fluorescence imaging after directly adding 1 μM Cy5-labelled complementary DNA strand onto the *C. glutamicum* cells for 1 h at 37°C. (c) Colocalization of the FAM-labeled 16:0-16:0-DNA conjugate with a Cy3-labelled non-complementary strand on the membrane of *C. glutamicum* cells. These cells were first incubated with 0.5 μM of the 16:0-16:0-DNA conjugate for 1 h at 37°C, after washing away the free probes, 1 μM of the non-complementary strand was then added and incubated for 30 min. The Pearson correlation coefficient was determined to be -0.029. Scale bar, 5 μm.

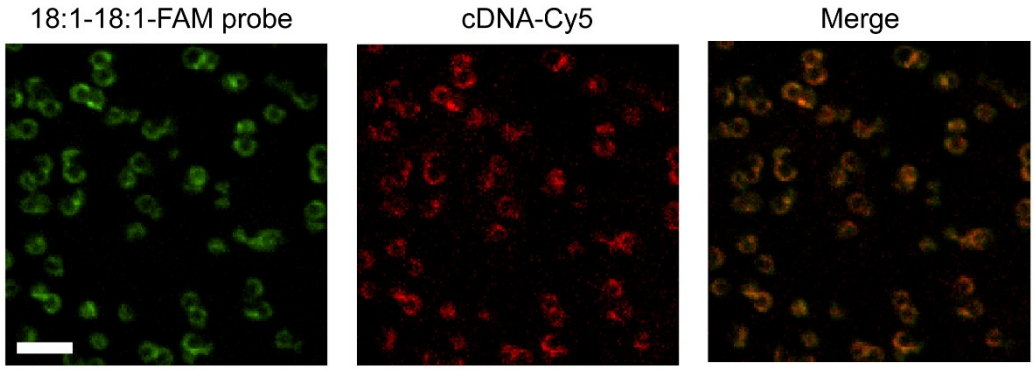

Figure S10. Colocalization of the FAM-labeled 18:1-18:1-DNA conjugate with a Cy5-labelled complementary strand on the membrane of *S. aureus* cells. These cells were first incubated with 1 μM of the 18:1-18:1-DNA conjugate for 1 h at 37°C, after washing away the free probes, 1 μM complementary strand was then added and incubated for 30 min. The Pearson correlation coefficient was determined to be 0.70.

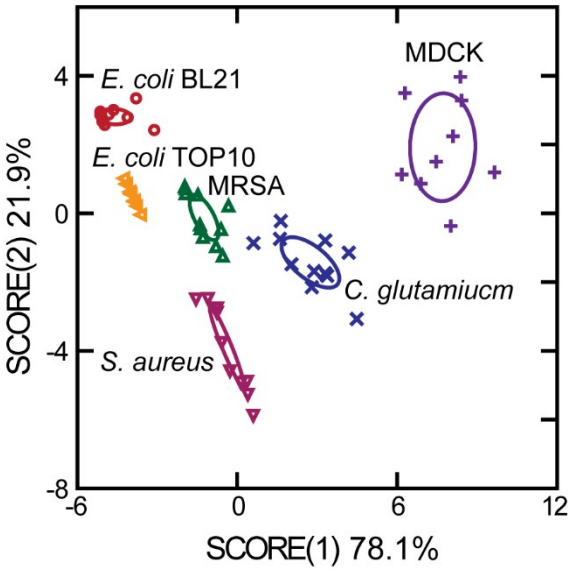

Figure S11. Linear discriminant analysis based on the fluorescence response pattern of the 18:1-18:1-DNA and cholesterol-DNA conjugates on five types of bacterial strains and MDCK cells. The transformed canonical scores were plotted with 95% confidence ellipses and 0.001 tolerance around the centroid of each group.

3. Supplementary Tables

Table S1. DNA sequences used in this study.

Name	Sequence (5'-3')
20 nt DNA	Lipid-TGATGTGGTGTGTGAGAGAG-FAM
80 nt DNA	Lipid-CTCCCTACCATCACCTCCACACAACTACCACCCACATCCCACTACTTCT CTCCACTTTTCACTCACATTTCACTCACCCT-FAM
Cy5-cDNA	CTCTCTCACACACCACATCA-Cy5
Cy3-ncDNA	Cy3-GAGTCCTCACACTTGCTTCGATTT-thiol-modifier C3

Table S2. Bacterial membrane modification percentage[#] of each lipid-DNA conjugate.

	E. coli TOP10	*E. coli* BL21	*P. aeruginosa*	*C. glutamicum*	*S. aureus*	*M. luteus*
18:1	84 ± 4.4	8.1 ± 0.9	<1.0	52 ± 5.5	87 ± 2.8	5.4 ± 0.5
18:0	3.9 ± 0.6	7.0 ± 1.4	<1.0	4.7 ± 0.8	5.5 ± 1.7	<1.0
Cholesterol	9.9 ± 0.9	10 ± 2.3	<1.0	71 ± 1.1	77 ± 3.7	11 ± 1.8
16:0-16:0	4.8 ± 0.4	13 ± 1.3	<1.0	94 ± 2.9	83 ± 2.1	<1.0
18:1-18:1	31 ± 1.9	6.7 ± 1.2	<1.0	88 ± 2.0	90 ± 1.2	8.8 ± 2.8
18:0-18:0	33 ± 3.2	17 ± 1.6	<1.0	90 ± 1.4	80 ± 5.2	<1.0

[#] Membrane modified bacteria were defined as those cells of membrane fluorescence intensities at least higher than the mean cellular autofluorescence signal plus 10-fold of the standard error of the mean, as measured from three imaging zones in each experiment. Here, to count both high and medium level membrane-modified cells, the threshold value was chosen different from that of Fig. 1c and 2c.

Table S3. Maximum bacterial membrane density of each lipid-DNA conjugate (unit: nm^{-2}).

	18:1	18:0	Cholesterol	16:0-16:0	18:1-18:1	18:0-18:0
E. coli TOP10	0.20 ± 0.01	0.06 ± 0.01	0.12 ± 0.01	0.10 ± 0.01	0.17 ± 0.01	0.15 ± 0.01
S. aureus	0.18 ± 0.01	0.06 ± 0.01	0.13 ± 0.01	0.26 ± 0.01	0.53 ± 0.02	0.62 ± 0.02
C. glutamicum	0.11 ± 0.01	0.05 ± 0.01	0.45 ± 0.01	0.71 ± 0.01	0.53 ± 0.10	0.57 ± 0.01

Table S4. Jackknife classification matrix of the 18:1-DNA- and 16:0-16:0-DNA-based array.

	E. coli BL21	*C. glutamicum*	MRSA	S. aureus	*E. coli* TOP10	**%correct**
E. coli BL21	11	0	0	0	0	100
C. glutamicum	0	11	0	0	0	100
MRSA	0	0	11	0	0	100
S. aureus	0	0	0	11	0	100
E. coli TOP10	0	0	0	0	11	100
Total	11	11	11	11	11	100

Table S5. Jackknife classification matrix of the cholesterol-DNA- and 18:1-18:1-DNA-based array.

	E. coli BL21	*C. glutamicum*	MDCK	MRSA	*S. aureus*	*E. coli* TOP10	**%correct**
E. coli BL21	11	0	0	0	0	0	100
C. glutamicum	0	10	0	1	0	0	91
MDCK	0	0	10	0	0	0	100
MRSA	0	0	0	11	0	0	100
S. aureus	0	0	0	0	11	0	100
E. coli TOP10	0	0	0	0	0	11	100
Total	11	10	10	12	11	11	98

Table S6. Normalized membrane fluorescence intensities of five bacterial strains and the MDCK cells for the linear discriminant analysis.

Five sample classification			Six sample classification		
Sample cells	**18:1-FAM**	**16:0-16:0-FAM**	**Sample cells**	**Cholesterol-FAM**	**18:1-18:1-FAM**
E. coli TOP10	0.1598	0.0457	*E. coli* TOP10	8.3432E-06	0.2354
E. coli TOP10	0.1495	0.0278	*E. coli* TOP10	6.1816E-06	0.2054
E. coli TOP10	0.1368	0.0423	*E. coli* TOP10	5.7846E-06	0.1813
E. coli TOP10	0.1319	0.0490	*E. coli* TOP10	5.2909E-06	0.2248
E. coli TOP10	0.1480	0.0332	*E. coli* TOP10	5.1012E-06	0.1661
E. coli TOP10	0.1439	0.0388	*E. coli* TOP10	4.5326E-06	0.1996
E. coli TOP10	0.1512	0.0336	*E. coli* TOP10	5.8333E-06	0.1798
E. coli TOP10	0.1385	0.0278	*E. coli* TOP10	5.3587E-06	0.2219
E. coli TOP10	0.1723	0.0329	*E. coli* TOP10	4.5461E-06	0.2245
E. coli TOP10	0.1763	0.0405	*E. coli* TOP10	4.2414E-06	0.2569
E. coli TOP10	0.1190	0.0288	*E. coli* TOP10	5.7394E-06	0.2044
S. aureus	0.1154	0.4285	*S. aureus*	0.0864	0.5250
S. aureus	0.1546	0.4795	*S. aureus*	0.0834	0.5245
S. aureus	0.1251	0.4091	*S. aureus*	0.0523	0.7782
S. aureus	0.1080	0.3910	*S. aureus*	0.0593	0.6991
S. aureus	0.1659	0.4630	*S. aureus*	0.0742	0.4960
S. aureus	0.1628	0.4050	*S. aureus*	0.0762	0.7037
S. aureus	0.1457	0.5414	*S. aureus*	0.0806	0.5333
S. aureus	0.1488	0.4186	*S. aureus*	0.0428	0.4844
S. aureus	0.1566	0.4748	*S. aureus*	0.0453	0.6642
S. aureus	0.1161	0.4338	*S. aureus*	0.0634	0.7301
S. aureus	0.1269	0.4773	*S. aureus*	0.0573	0.5988
C. glutamicum	0.0555	0.7209	*C. glutamicum*	0.4028	0.5696
C. glutamicum	0.0447	0.7390	*C. glutamicum*	0.3523	0.5836
C. glutamicum	0.0376	0.7298	*C. glutamicum*	0.4413	0.5043
C. glutamicum	0.0493	0.8947	*C. glutamicum*	0.4047	0.5771
C. glutamicum	0.0339	0.7253	*C. glutamicum*	0.3278	0.4531
C. glutamicum	0.0540	0.6105	*C. glutamicum*	0.3274	0.5161
C. glutamicum	0.0565	0.6555	*C. glutamicum*	0.3508	0.4182
C. glutamicum	0.0278	0.6139	*C. glutamicum*	0.3770	0.5540
C. glutamicum	0.0228	0.6341	*C. glutamicum*	0.4871	0.5538

C. glutamicum	0.0567	0.7538	*C. glutamicum*	0.4297	0.6948
C. glutamicum	0.0883	0.7422	*C. glutamicum*	0.2553	0.4334
E. coli BL21	0.0109	0.0870	*E. coli* BL21	0.0134	0.0310
E. coli BL21	0.0102	0.0150	E. coli BL21	0.0174	0.0305
E. coli BL21	0.0030	0.0043	*E. coli* BL21	0.0190	0.0151
E. coli BL21	0.0069	0.0111	E. coli BL21	0.0378	0.0240
E. coli BL21	0.0070	0.0411	*E. coli* BL21	0.0152	0.0408
E. coli BL21	0.0086	0.0158	E. coli BL21	0.0196	0.0101
E. coli BL21	0.0186	0.1778	*E. coli* BL21	0.0160	0.0159
E. coli BL21	0.0134	0.0434	E. coli BL21	0.0825	0.0504
E. coli BL21	0.0175	0.1293	*E. coli* BL21	0.1355	0.1036
E. coli BL21	0.0113	0.1162	E. coli BL21	0.1265	0.0208
E. coli BL21	0.0127	0.1031	*E. coli* BL21	0.0551	0.0204
MRSA	0.0892	0.2284	MRSA	0.1466	0.2474
MRSA	0.0592	0.2348	MRSA	0.1400	0.2621
MRSA	0.0857	0.2711	MRSA	0.1887	0.3714
MRSA	0.0700	0.3257	MRSA	0.1332	0.3678
MRSA	0.0531	0.2497	MRSA	0.1558	0.4002
MRSA	0.0705	0.2799	MRSA	0.1618	0.4264
MRSA	0.0641	0.3266	MRSA	0.1702	0.2780
MRSA	0.0448	0.2552	MRSA	0.1459	0.2526
MRSA	0.0398	0.2739	MRSA	0.1372	0.3488
MRSA	0.0588	0.1627	MRSA	0.1401	0.3399
MRSA	0.0442	0.2646	MRSA	0.2351	0.3323
			MDCK	1.3453	0.3129
			MDCK	0.8177	0.2940
			MDCK	0.9783	0.3203
			MDCK	0.9537	0.3687
			MDCK	0.7520	0.4922
			MDCK	0.7141	0.4534
			MDCK	0.7788	0.6085
			MDCK	0.9532	0.5475
			MDCK	0.8898	0.4313
			MDCK	0.8170	0.4644

References

1. Y. Bagheri, S. Chedid, F. Shafiei, B. Zhao and M. You, *Chem Sci*, 2019, **10**, 11030-11040.
2. W. Lin, C. Yu, S. Triffo and J. T. Groves, *Curr Proc Chem Biol*, 2010, **2**, 235-269.